Journal of Testing and Evaluation, Sept 2005 Vol. 2, No. 8
Paper ID:JAI12957
Available online at: www.astm.org

C.T. Scott, R. Hernandez, C. Frihart, R. Gleisner, and T. Tice[1]

Method for Quantifying Percentage Wood Failure in Block-Shear Specimens by a Laser Scanning Profilometer

ABSTRACT: A new method for quantifying percentage wood failure of an adhesively bonded block-shear specimen has been developed. This method incorporates a laser displacement gage with an automated two-axis positioning system that functions as a highly sensitive profilometer. The failed specimen is continuously scanned across its width to obtain a surface failure profile. The laser is then moved incrementally along the length of the specimen and repeatedly scanned to obtain a three-dimensional digital profile of the surface. This digital profile can then be reconstructed and analyzed with appropriate software. Special algorithms are used to quantify percentage wood failure and degree of wood failure (depth of wood failure) and to recognize various surface anomalies, such as bondline voids (air bubbles). This paper presents exploratory data on several different types of wood failure and correlates these measurements to visual inspections of experienced observers. The device is very sensitive to most observed failures, particularly those with deep wood failure. However, shallow failures close to the bondline can be problematic. The algorithms allow a "roughness" tolerance to be specified to characterize these surfaces. This new method will be useful for automating measurement of wood failure in block-shear specimens with good precision and repeatability.

KEYWORDS laser, profilometer, adhesion, block-shear, wood failure

Introduction

Quantifying percentage wood failure of an adhesively bonded block-shear specimen is a challenging process and requires a highly trained observer to make a visual estimate of total wood failure on the shear cross section with an estimate of shallow and deep wood failure to the nearest 5%, as specified in the ASTM D 5266 standard [1]. Generally, wood failure estimators do not have difficulty with very high or very low percentages of wood failure. However, difficulty occurs in the middle "pass–fail" range (30% to 80% wood failure), where accuracy is most critical, depending on the adhesive requirements. Visual estimates of wood failure within this range can be interpreted very differently among several observers [2]. The development of new techniques to automate this process would greatly improve and expedite these determinations.

---

[1] General Engineer, Research Engineer, Project Leader, Physical Science Technician, and Student, respectively, USDA Forest Service, Forest Products Laboratory, One Gifford Pinchot Drive, Madison, WI 53726 USA

Recently, researchers have developed an image analysis technique to estimate percentage wood failure on block-shear specimens [3]. This technique utilizes a digital camera to capture an image of the specimen surface, which is manipulated with appropriate software to calculate percentage wood failure. However, with imaging-based techniques, it is necessary to develop contrast between the bondline and the wood so that the two can be distinguished. This can be accomplished by adding colorants or dyes to the adhesive. A distinct advantage of this method is that it can be readily automated. However, it is not possible to differentiate between shallow and deep wood failure.

Our goal was to investigate the viability of an automated laser-scanning profilometer to quantify both percentage wood failure and degree of wood failure on block-shear specimens. Laser displacement sensors are sensitive to very small displacements and may be useful in detecting surface irregularities found on failed block-shear specimens. This paper presents a method whereby a laser displacement sensor is incorporated in a two-axis positioning system to scan the surface of a failed block-shear specimen. We attempted to evaluate the accuracy of this method compared with failure estimates made by trained observers and identified specimen characteristics that require a more complex analysis approach.

Experimental

Five previously tested block-shear specimens were selected for this analysis (Figs. 1 to 3). These specimens were produced from 25-mm hard maple blocks according to the ASTM D 905 [4] standard and represented a diverse range of wood failures and contained several unique surface features that could pose some difficulty in visual grading. All specimens had undergone durability treatment (vacuum–pressure water soak) and were tested wet. These specimens were visually graded by five observers according to the guidelines of ASTM D 5266, and the results for percentage wood failure were tabulated.

A laser profilometer was designed to probe the surface of a failed block-shear specimen (Fig. 4). This device incorporates a high-resolution laser displacement sensor with an automated two-axis positioning system. The block-shear specimen was placed under the laser, and stepper motors controlled by timed relays were used to incrementally scan the surface. Laser location was measured with a linear variable differential transducer (LVDT) on each axis. Data acquisition was configured to capture sensor output at the rate of 30 Hz. To accurately reproduce the surface profile, about 1,000 laser sensor readings were acquired across the width of the specimen (about 25 μm between readings) for about 25 equally spaced increments (1 mm each) along the length (Fig. 5). An NAIS-ANL 2300 Laser with an LM200 Analog Sensor was used to measure surface topography. This laser has a spot size of about 25 μm diameter with a displacement resolution of about 13 μm.

Data were manipulated and analyzed to produce an accurate three-dimensional digital profile of the surface topography. For quantitative analysis, data were imported to a spreadsheet, smoothed to remove noise from the LVDTs, and sorted to remove edge effects. Because there was considerable warp in all specimens due to the durability test, a parabolic function was fit to this distortion and subtracted from the raw data to produce a “flat” bondline. The data were then sorted to produce a cumulative frequency distribution for determining degree of wood failure. Conceptually, the bondline could thus be located within a prescribed tolerance with the percentages of shallow and deep wood failure characterized by defining the corresponding wood failure depths.

Results

The laser scanning profilometer seemed to function adequately for our purposes. The reflectivity of the failure surface was sufficient to give excellent resolution. However, one of the principal assumptions of this technique is how concentrated the grid pattern would need to be to adequately recreate the failure surface. Because the laser spot size is only 25 µm and the increment selected was 1 mm, only 2.5% of the surface was actually being profiled. To validate this assumption qualitatively, it was necessary to convert the digital coordinates to contour plots and “virtually” recreate the failure surface (Figs. 6, 7). For this purpose, the date were smoothed by averaging every fifth point. The virtual representations could then be visually compared to the original (compare Figs. 6 and 7 to Fig. 5).

An unexpected complication that compromised the objectivity of the method was the presence of warp (cup and bow) developed in the specimens after a vacuum–pressure soak. In most cases, the magnitude of cup (across the width) was significantly greater than the surface irregularities (Fig. 8). It was reasonable to assume that the cup would remain consistent along the length of the specimen, so a parabolic function was fit to this distortion and subsequently subtracted from the raw data to produce a “flat” bondline. This assumption worked well for all but one of the specimens, which had significant bow in addition to cup. Once the warp was removed from the data (Fig. 9), it was possible to sort the laser sensor data by distance to the bondline to produce a frequency distribution for wood failure (Fig. 10).

At this point in the analysis, it was necessary to define a tolerance for bondline thickness, whereby all data within this tolerance would be considered to be within the bondline and all data outside this tolerance would be considered wood failure. Furthermore, a second tolerance would need to be specified to define “shallow” wood failure to distinguish it from “deep” wood failure (Fig. 10). For the specimens evaluated in this study, tolerances of ±40 and ±60 µm were selected for both the bondline thickness and shallow wood failure. (Typical bondline thickness is about 80 µm, and the thickness of a small fiber bundle, two to five fibers, is 40 to 60 µm.) Table 1 summarizes the results from this analysis as well as the visual grading values obtained from the trained observers.

Specimens 1 and 5 (Fig. 1) seemed to be obvious adhesive failures. However, one of the observers interpreted the degree of failure in specimen 5 quite differently from the others. In this case, some regions had considerable fiber pullout. Does this constitute shallow wood failure? The profilometer analysis also shows a small degree of shallow wood failure for the tolerances specified. However, specimen 5 was also the specimen that had significant bow in addition to cup, which may have compromised the analysis.

Specimens 2 and 3 (Fig. 2) were examples of the more problematic failure surfaces to characterize visually. These observations varied widely for both, as was anticipated. Specimen 2 appeared to have considerable wood failure. However, upon closer inspection, most of the wood failures were tall, narrow ridges of fiber pullout, with exposed regions of bondline in between. This may have caused an observer to overestimate the degree of wood failure. Conversely, specimen 3 has broader regions of wood failure and adhesive failure, but gave similar results.

Finally, specimen 4 (Fig. 3) has very obvious and severe wood failure. All observers recognized this severity and yet the visual ratings still varied by as much as 40%. The profilometer ratings were more consistent and effectively differentiated shallow wood failure from deep wood failure.

Conclusions

The laser-scanning method accurately reproduced graphical representations of the surface failure topography in a variety of block-shear specimens. It was also effective in differentiating shallow and deep wood failure, as called for in the ASTM D 5266 standard. The laser displacement sensor appeared to adequately resolve a variety of surface irregularities, and the grid pattern prescribed appeared to be sufficient to reconstruct a digital contour of the actual surface. Ideally, this method would be fairly simple to implement on flat specimens. However, all the specimens tested contained significant degrees of warp due to the effects

Table 1—Percentage wood failure determined by ASTM D method, and by laser-scan method

	Percentage wood failure determined by each reviewer					**Percentage wood failure determined by laser-scan method**	
Specimen number	A	B	C	D	E	Tolerance ± 40µm Total (shallow/deep)	Tolerance ±60µm Total (shallow/deep)
01	0	0	0	0	0	12 (12/0)	2 (2/0)
02	75	65	75	80	10	44 (24/20)	30 (21/9)
03	70	40	30	45	95	52 (23/29)	37 (16/21)
04	60	90	80	90	100	77 (13/64)	70 (11/59)
05	0	0	0	5	85	38 (25/13)	22 (18/4)

of a vacuum–pressure soak test. In many specimens, the magnitude of warp was several times that of the surface irregularities. Therefore, it was necessary to “flatten” the bondline by fitting a parabolic function to the warp and subtracting it from the raw data. A thickness tolerance could then be specified to define the bondline region as well as a region of shallow wood failure.

Specimen 5 was particularly problematic because it contained significant distortion (both cup and bow). Fitting a parabolic function to the cup and subtracting the function from all the scans was not sufficient to reproduce a flat bondline. This specimen had obvious regions of bondline voids that should have been readily recreated by the laser-scanning method. Therefore, it may be necessary to fit a bi-quadratic function to the surface to expose these features and improve the analysis.

When compared with round-robin evaluations, we found that the laser-scanning method fell within the range of observations of visual estimates for percentage wood failure, although some of these estimates varied widely. The laser-scanning method could, however, account for small regions of bondline and shallow wood failure that were not readily recognized in visual observations. This attribute should greatly improve the discrimination capabilities of the method to distinguish the intermediate, mixed failures that are most critical for determining adhesive performance.

References

[1] “Standard Practice for Estimating the Percentage of Wood Failure in Adhesive Bonded Joints,” ASTM D 5266, American Society for Testing and Materials, West Conshohocken, PA, June 1999.
[2] “Wood Failure Round Robin Report,” CSA/A37O/SC05.3, Canadian Standards Association, Mississauga, Ontario, August 2002.
[3] Zink, A.G. and Kartunova, E., “Wood Failure in Plywood Shear Samples Measured with Image Analysis,” Forest Prod. J. 48(4):69-74, April 1998.
[4] “Standard Test Method for Strength Properties of Adhesive Bonds in Shear by Compression Loading,” ASTM D 905, American Society for Testing and Materials, West Conshohocken, PA, October 2003.

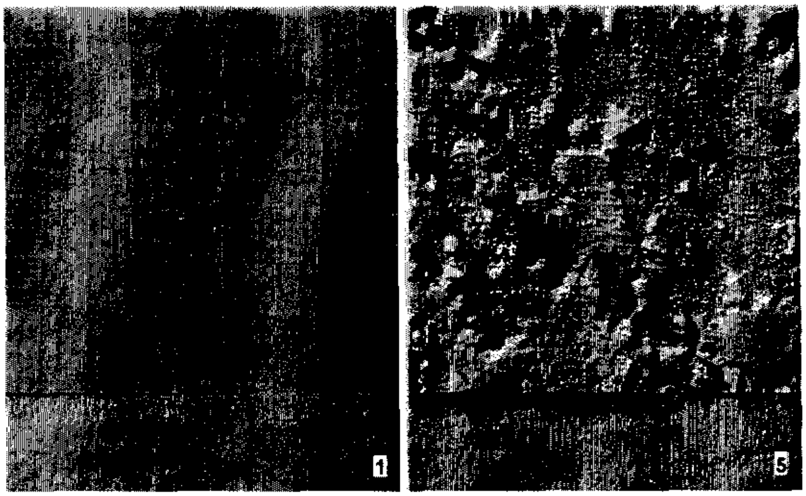

Figure 1. Specimens 1 and 5 showing different degrees of adhesive failure. Specimen 5 appears also to have large bondline voids.

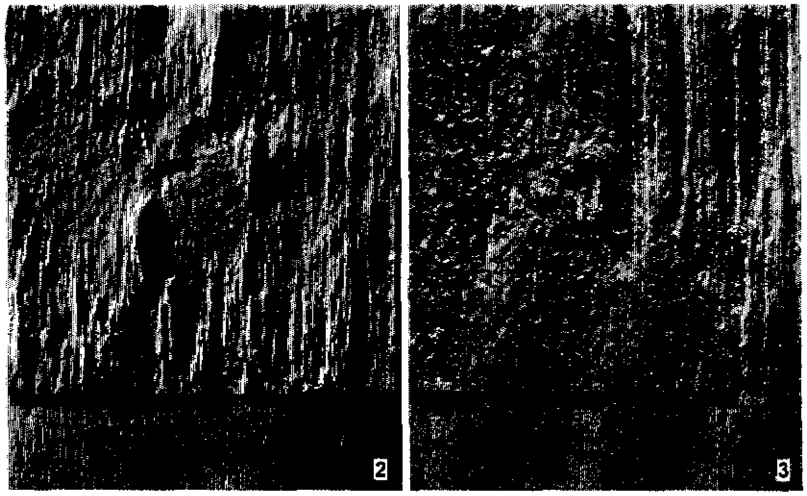

Figure 2. Specimens 2 and 3 show mixed levels of bondline, shallow, and deep wood failure.

Figure 3. Specimen 4 shows severe wood failure extending well beyond the bondline.

Figure 4. Laser beam probing the surface of specimen 4.

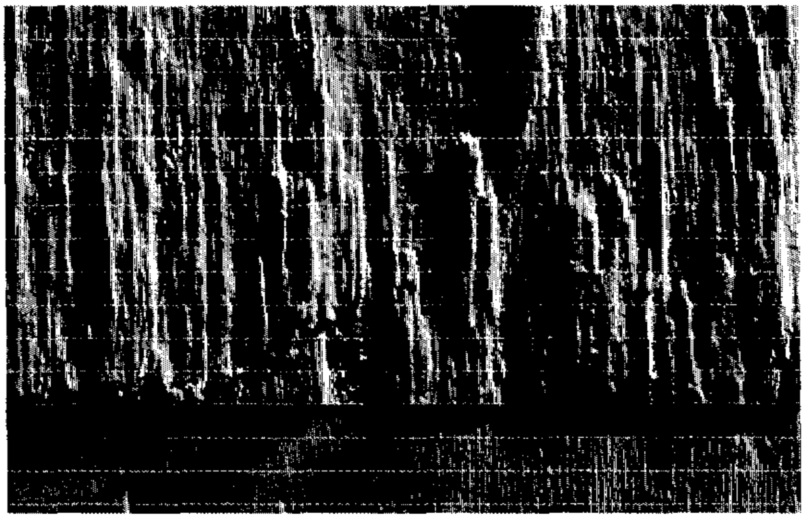

Figure 5. Location of the beam grid used to recreate the surface of specimen 2.

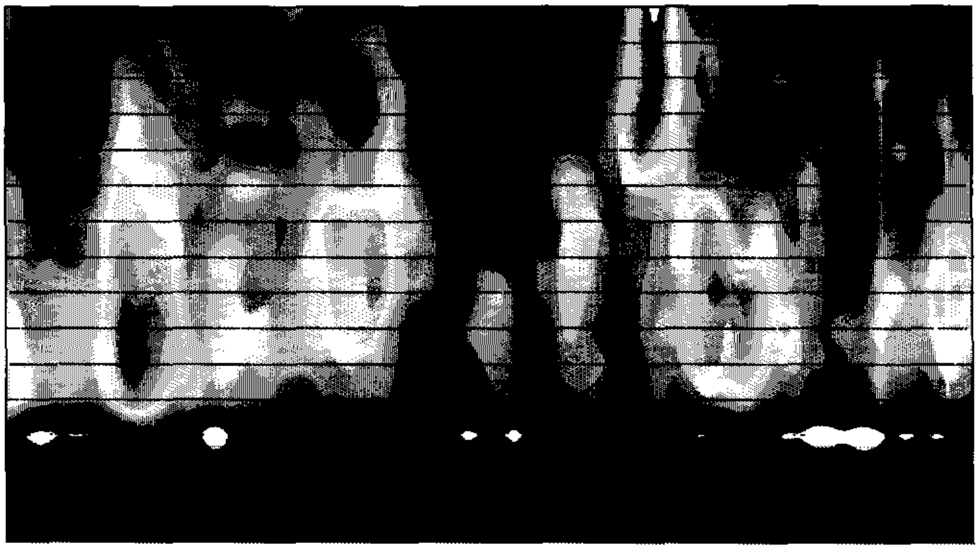

Figure 6. Two-dimensional digital contour plot of specimen 2.

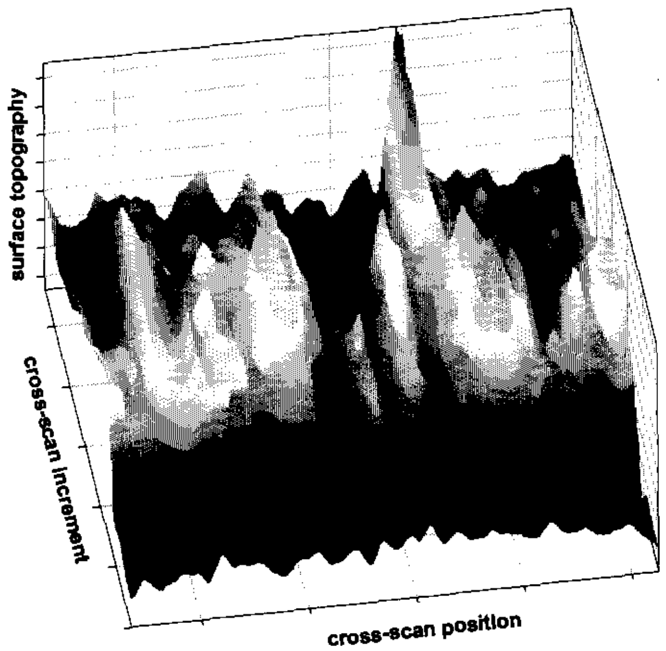

Figure 7. Three-dimensional digital contour plot of specimen 2.

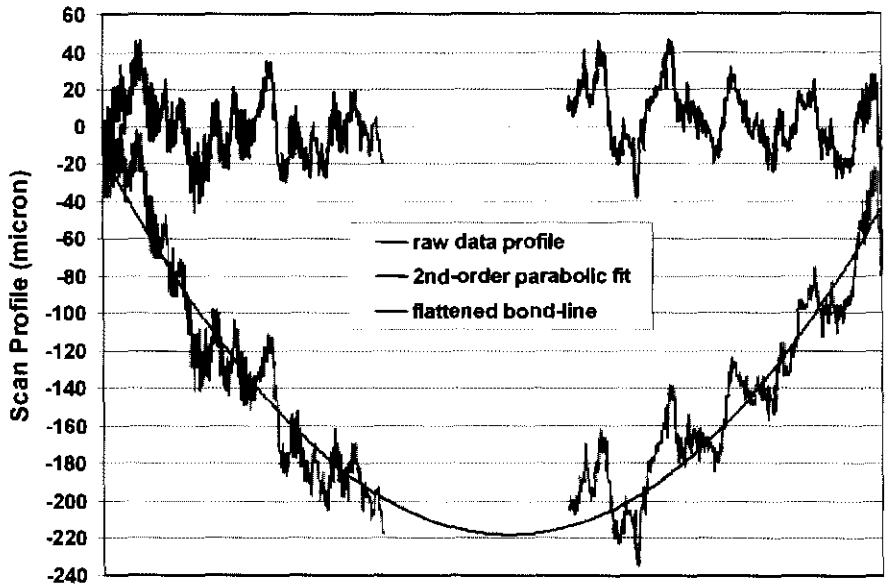

Figure 8. Typical single-scan profile for specimen 4 before and after flattening. The gap in the data represents the hole visible on the cut surface.

Figure 9. End-view representation of the surface of specimen 4 after flattening the bondline.

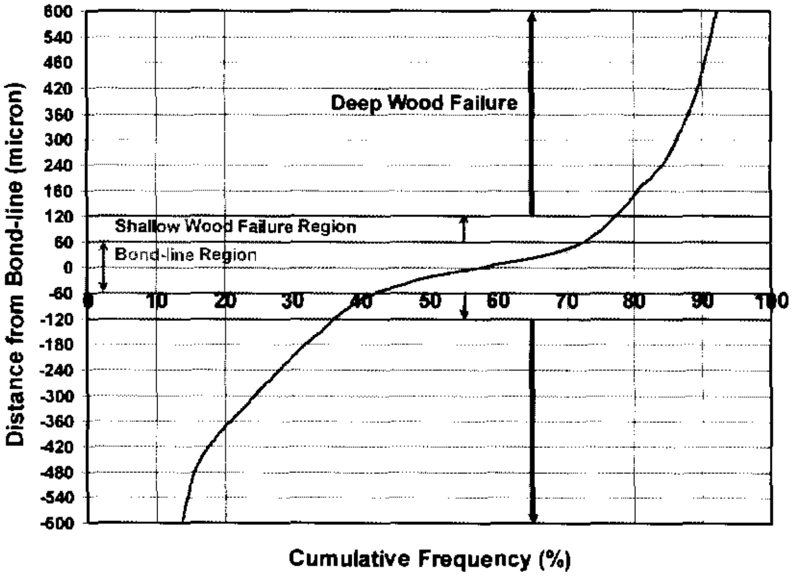

Figure 10. Cumulative frequency distribution of wood failure for specimen 4 denoting the bondline tolerance and the shallow wood failure tolerance.